Molecularly Imprinted Polymeric Receptors with Interfacial Hydrogen Bonds for Peptide Recognition in Water

*Milad Zangiabadi and Yan Zhao**

Department of Chemistry, Iowa State University, Ames, Iowa 50011-3111

zhaoy@iastate.edu

RECEIVED DATE

ABSTRACT. Protein receptors bind their peptide ligands by a combination of hydrophobic and hydrogen-bonding interactions to achieve high affinity and selectivity. Construction of synthetic receptors for peptides by the same principle, however, is challenging because of the complexity of the guest molecules and subtle structural differences among closely related sequences. Molecular imprinting of peptides in surface–core doubly cross-linked micelles yielded hydrophobic pockets complementary to the hydrophobic side chains of peptides. Amide-functionalized bisacrylamide cross-linkers such as N,N'-methylenebisacrylamide (MBAm) used in the core-cross-linking installed a layer of hydrogen bonds at the surfactant/water interface and was found to enhance the molecular recognition of peptides in water, particularly hydrophilic ones rich in polar residues. An extremely strong imprinting effect was obtained, with the imprinted/nonimprinted ratio ranging from 3000 to 10000 for model tripeptides. These hydrogen bonds allowed distinction of closely related peptide sequences and enabled a general, simple, one-pot

preparation of highly selective receptors for binding complex hydrophilic peptides with <200 nM affinity in aqueous buffer.

Key words: molecular imprinting, binding, peptide, molecular recognition, micelle, cross-linker

Introduction

Peptides (and their longer congener proteins) are one of the most important classes of biomolecules and their recognition by biogenic receptors is vital to many biological processes. Motivated by this significance, chemists over the last decades used many platforms to build synthetic receptors for peptides, as discussed in several representative reviews.[1-3]

A difficult challenge in peptide recognition is derived from the complexity and sheer size of the guest molecule. A biological peptide with a dozen or more residues contains an enormous amount of supramolecular information. It is a daunting task if one wants to build complementary features on a preorganized receptor to accurately match such a guest in hydrogen-bonding, hydrophobic, and ionic groups.

Whereas design and synthesis of molecular receptors become too complex to be practical in such a scenario, an alternative approach—molecular imprinting—is available, to build binding sites directly around guest molecules.[4,5] In the latter technique, the peptide of interest is used as a template and mixed with a large amount of a cross-linker and suitable functional monomers (FMs) that bind the template molecule by noncovalent or reversible covalent bonds. Cross-linking creates a polymeric network around the template. Removal of the template vacates the imprinted site with size, shape, and binding groups ideally complementary to the template molecule. The technique, in combination with precipitation polymerization, allowed Shea and co-workers to produce excellent receptors for several biological peptides,[6] with those built for mellittin (the major component of bee venom) capable of removing the toxin from the bloodstream of living mice.[7] It should be noted that peptide-imprinted materials not only can recognize the templating peptides but also proteins if a specific sequence of a protein is used as the

template. This latter approach, termed epitope imprinting, has found many applications since its inception.[8-17]

An ideal receptor for peptide should be simple to prepare, and applicable to peptides of different size, hydrophobic and hydrophilic alike. The binding must be able to occur in aqueous solution, with biologically useful binding affinities. High binding selectivity is essential to biological applications, which demand receptors to distinguish closely related sequences. Despite the progress made over the years, a general method in peptide recognition is lacking and most reported receptors fall short in one or multiple of the above criteria.[1-3]

Herein, we report a facile method to synthesize water-soluble polymeric nanoparticles for peptide recognition in water. These protein-sized receptors were prepared through molecular imprinting in doubly cross-linked micelles in a one-pot reaction. Amide-functionalized free radical cross-linkers were found to be particularly effective in enhancing the molecular recognition, through formation of a layer of hydrogen bonds at the surfactant/water interface. Closely related sequences were differentiated, and receptors for complex biological peptides were made as easily as those for simple model peptides, with 110–170 nM binding affinities.

Results and Discussion

Design and Synthesis of Peptide-Binding MINPs. The best receptors of peptides are found in nature and their binding mechanisms can guide our design of synthetic receptors. Figure 1 shows the crystal structure of a complex between GABARAP and its main binding epitope on calreticulin, a chaperone located in the endoplasmic reticulum.[18] The former is a ligand-gated chloride-channel protein controlled by the neurotransmitter 4-aminobutyrate (GABA). The epitope, with a sequence of SLEDDWDFLPP, has a number of notable hydrophobic (W, F, L, P) and hydrophilic residues (S, E, D). Also noticeable in the crystal structure is that the binding relies on combined hydrophobic and polar interactions, hydrogen bonds mainly in the latter. While the indole ring of Trp6 and the isobutyl group of Leu9 on the epitope insert themselves into the matching hydrophobic pockets on the GABARAP formed through folding of

the peptide chain, multiple hydrogen bonds are engaged simultaneously between the host and the guest, as indicated by the solid green lines.

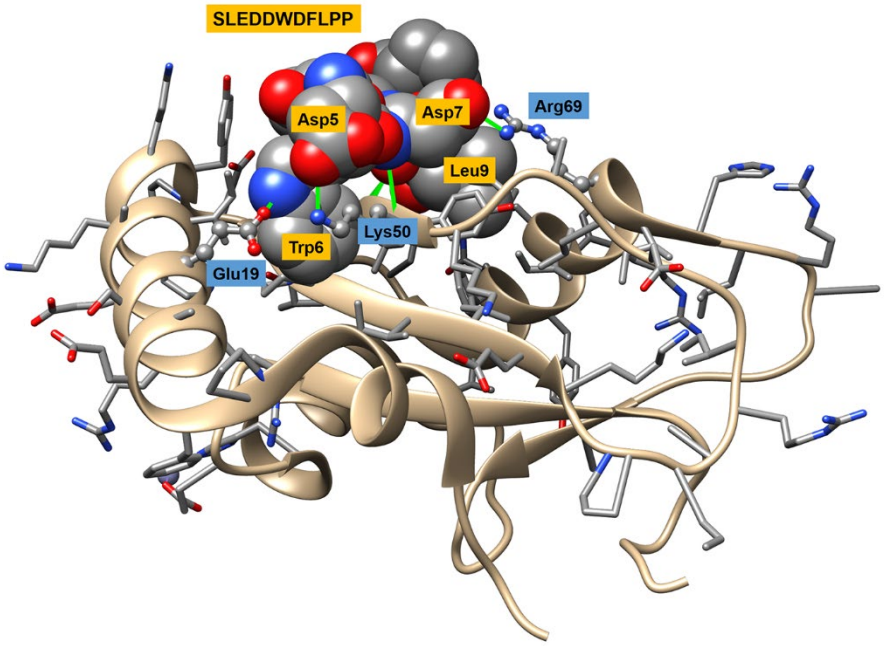

Figure 1. Crystal structure of GABA type A receptor in complex with its binding epitope, with the latter shown as a CPK model. Structural data were obtained from the Protein Data Bank (ID: 3DOW). Molecular graphics was created using UCSF Chimera.[19]

Complementarity in combined hydrophobic and polar interactions is by no means an isolated incident in biology, and has been recognized as the key reason for protein–protein[20] and protein–ligand interactions.[21] The main challenge is in the construction of suitable scaffolds to embody such complementarity in an accurate and efficient manner for complex guests such as peptides.

Scheme 1 shows our strategy to create a receptor with simultaneous complementarity in hydrophobicity and hydrogen-bonding to a peptide guest, through molecular imprinting of surfactant micelles.[22] In the first step, a peptide—with its hydrophobic side chains represented by the purple shapes along the green peptide backbone—was solubilized in water by the micelle of cross-linkable surfactant **1**, together with 2,2-dimethoxy-2-phenylacetophenone (DMPA, a photoinitiator) and a free radical cross-linker—divinyl benzene (DVB) or **4**–**9**.[23] Addition of Cu(II), sodium ascorbate, and diazide **2** cross-linked the surface of

the micelle through the Cu(I)-catalyzed click reaction. The resulting surface-cross-linked micelle (SCM) was functionalized by another round of click reaction using monoazide **3**. UV irradiation initiated free radical polymerization/cross-linking of the micellar core among the methacrylate of **1** and DVB (and/or **4**–**9**). Progress of the reaction was monitored by ^{1}H NMR spectroscopy and dynamic light scattering (DLS) (Figures S1–S4). The resulting molecularly imprinted nanoparticles (MINPs) were purified simply by pouring the aqueous reaction mixture into acetone and washing the precipitate with organic solvents, with the noncovalently bound template removed during the process. MINPs were typically ~5 nm in diameter as measured by dynamic light scattering (DLS), with an estimated M.W. of 50,000–60,000 Da (Figures S2 and S4). The DLS size was confirmed by transmission electron microscopy (TEM), as shown in Figure S5. The number of binding site per nanoparticle is controlled by the surfactant/template ratio. A 50:1 surfactant/template ratio, for example, affords an average of one binding site per nanoparticle, since the molecular weight of MINP translates to ~50 cross-linked surfactants.[22,24]

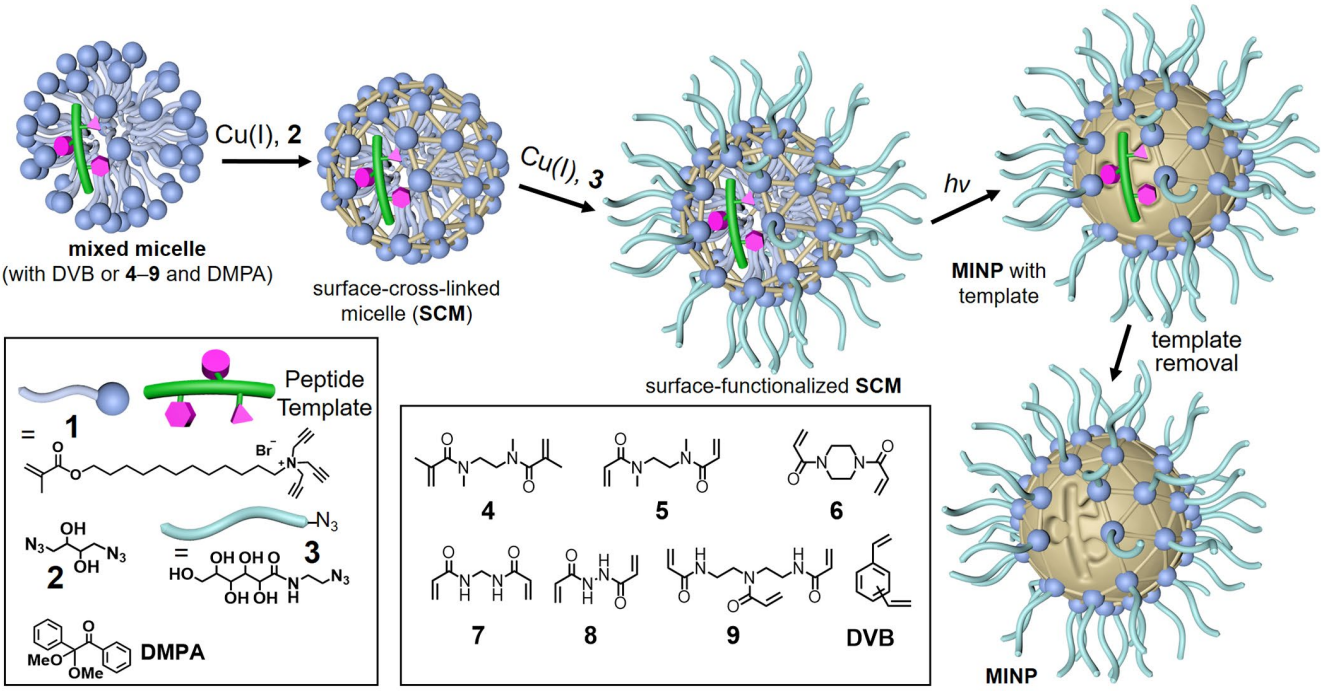

Scheme 1. Preparation of peptide-binding MINP by surface–core double cross-linking of the peptide-containing micelle of **1**.

One important feature of MINP is its modularity in synthesis. To introduce hydrogen-bonding capabilities, we hypothesized that amide-containing cross-linkers (**4**–**9**) would suffice. Essentially, the

polar groups on the peptide template would interact with the amides while the hydrophobic side chains insert themselves into the nonpolar core of the micelle. Cross-linking would then create imprinted hydrophobic pockets for the hydrophobic side chains and hydrogen-bonding sites for the polar groups simultaneously.

Our choice of **4**–**9** was based on several considerations. Compounds **4** and **5** differ in the polymerizable group, methacrylamide versus acrylamide. Whereas both **4** and **5** are fairly flexible, **6** is more rigid (and more hydrophobic) with the ring structure. In molecular imprinting, it is known that a balanced rigidity is ideal, at least for conventional imprinted polymers.[25] Compound **7**, N,N'-methylenebisacrylamide (MBAm) is commercially available. Its difference with **4**–**6** lies in the shorter tether between the two polymerizable groups and the presence of secondary amides. The former feature translates to a higher cross-linking density near the hydrogen-bonding sites. The latter affects the hydrogen-bonding capabilities of the cross-linkers: whereas **4**–**6** only contain hydrogen-bond acceptors, **7** has both donors and acceptors. Compound **8** is similar to **7**, but has an even tighter structure. Compound **9** has three instead of two cross-linkable acrylamides, with mixed hydrogen-bond donors and acceptors. Finally, DVB, a common free radical cross-linker serves as the control, without any amide bonds.

Evaluation of Amide-Containing Cross-Linkers. Our first model peptide was RWW, having a hydrophilic guanidinium side chain and two large hydrophobic indoles from the tryptophans. As shown in Table 1, MINP prepared with 1 equiv DVB to the cross-linkable surfactant bound the templating peptide with an association constant of K_a = 14.2 $\times 10^5$ M^{-1} (entry 1) by isothermal titration calorimetry (ITC). ITC is the most reliable method to study intermolecular interactions[26] and ITC-measured binding constants of MINPs have been validated previously with fluorescence spectroscopy.[24]

Table 1. Binding data for MINPs prepared with different core-cross-linkers.

Entry	template	Guest	Cross linker	K_a ($\times 10^5$ M^{-1})	-ΔG (kcal/mol)	-ΔH (kcal/mol)	TΔS (kcal/mol)
1	RWW	RWW	DVB	14.2 ± 1.3	8.39	19.24 ± 1.2	-10.85
2	RWW	RWW	**4**	9.15 ± 0.1	8.13	14.89 ± 0.5	-6.76

3	RWW	RWW	**5**	9.29 ± 0.1	8.14	18.36 ± 1.0	-10.22
4	RWW	RWW	**6**	8.81 ± 0.5	8.10	13.35 ± 1.9	-5.25
5	RWW	RWW	**7**	11.1 ± 1.6	8.24	17.49 ± 0.5	-9.25
6	RWW	RWW	**8**	7.79 ± 0.3	8.03	14.46 ± 1.6	-6.43
7	RWW	RWW	**9**	6.81 ± 0.6	7.95	12.57 ± 1.9	-4.62
8	RWW	RWW	DVB & **7**	8.86 ± 0.4	8.11	13.68 ± 0.6	-5.75
9	None[b]	RWW	**7**	< 0.003	-	-	-
10	WKK	WKK	DVB	3.31 ± 0.1	7.52	11.89 ± 2.4	-4.37
11	WKK	WKK	**4**	7.67 ± 0.4	8.02	12.19 ± 0.5	-4.17
12	WKK	WKK	**5**	7.92 ± 0.7	8.04	12.34 ± 0.4	-4.30
13	WKK	WKK	**6**	8.45 ± 0.7	8.08	13.67 ± 0.5	-5.59
14	WKK	WKK	**7**	17.8 ± 6.6	8.52	22.92 ± 0.9	-14.4
15	WKK	WKK	2 equiv **7**	8.17 ± 0.5	8.06	12.89 ± 0.3	-4.83
16	WKK	WKK	**8**	6.59 ± 0.6	7.93	9.48 ± 0.5	-1.55
17	WKK	WKK	**9**	6.91 ± 0.7	7.96	10.66 ± 1.1	-2.70
18	WKK	WKK	DVB & **7**	11.4 ± 2.5	8.26	17.77 ± 0.5	-9.51
19	None[b]	WKK	**7**	< 0.006	-	-	-

[a] Ttrations were performed in HEPES buffer (10 mM, pH 7.4) in duplicates at 298 K and the errors between the runs were <10%. One equivalent of the cross-linker was used to the cross-linkable surfactant in the MINP preparation unless indicated otherwise in entry 14.[b] Nonimprinted nanoparticles (NINPs) were prepared without any template. Binding was very weak and the binding constant was estimated from ITC titration. Binding was very weak and the binding constant was estimated from ITC titration (Figure S6j and S7j).

In micellar imprinting, it is crucial that the free radical core-cross-linking, which sets the polymeric network around the template, takes place within the confined nanospace of the SCM.[27] Hence, we had some concerns at the outset of the project, especially for water-soluble cross-linkers such as **7** and **8** because polymerization might take place outside the micelle in the aqueous phase. What was encouraging in the amide-functionalized MINPS was that no insoluble materials (e.g., hydrogel) were observed during the preparation and the MINPs showed the normal size (~ 5 nm) by DLS (Figures S2 and S4). Thus, uncontrolled polymerization of the cross-linker outside the micelle was not a problem. Since the radical

initiator (DMPA) was hydrophobic and had a strong preference to reside within the nonpolar core of the micelle, our explanation was that, once the initiating radical reacted with the methacrylate of the cross-linkable surfactant (**1**) in the surface-cross-linked-micellar core, the propagating radical was covalently attached to the micelle and could only polymerize those cross-linker molecules located near the surfactant/water interface of the micelle (either due to their amphiphilicity or by diffusion if the cross-linker was water-soluble). Essentially, as long as the radical initiator was strongly hydrophobic, water-soluble cross-linkers (or monomers) had little chance being polymerized away from the micelle.

Although no uncontrolled polymerization outside the micelle seemed to happen, the amide cross-linkers produced MINPs with consistently weaker binding than the MINP cross-linked with DVB (entries 1–7). Combining DVB with the amide cross-linker did not help either, at least for **7** (entry 8). If anything, the combination was counterproductive, because the binding constant of the MINP made with DVB and MBAm decreased from that made with either cross-linker.

Not deterred by the apparent failure, we switched the template to WKK, a more hydrophilic peptide with one hydrophobic tryptophan and two hydrophilic lysines. The DVB-derived MINP(WKK) bound its template with a $K_a = 3.31 \times 10^5$ M^{-1} (entry 10), weaker than that of RWW by MINP(RWW). The result was reasonable, given that MINP binding in water has a strong hydrophobic driving force[22,24] and hydrophobic interactions are known to be proportional in strength to the hydrophobic surface area buried upon binding.[28]

To our delight, all the amide-functionalized MINPs outperformed the DVB-cross-linked MINP (entries 11–17), with the best result obtained with the commercially available MBAm (entry 14). It was exciting that a simple change of the core-cross-linker from DVB to MBAm increased the binding of RWW over 5-fold. Interestingly, using a higher level of the cross-linker did not help (entry 15) and using a combination of DVB and **7** was worse than using **7** alone but better than using DVB only (entry 17). Lastly, nonimprinted nanoparticles (NINPs) were prepared with MBAm as the cross-linker and their binding for RWW and WKK was extremely weak (entries 9 and 19). The MINP/NINP ratio, i.e., the

imprinting factor, was >3700 for RWW and >3000 for WKK, testifying to the strong imprinting effect in the cross-linked micelles.

Why is DVB better for the more hydrophobic RWW, while MBAm better for the hydrophilic WKK? The most likely reason is the different driving force involved in the binding. For a largely hydrophobic peptide, the dominant driving force for binding is hydrophobic interactions.[22,24] To maximize the binding interactions, well-formed hydrophobic pockets need to be constructed in the nonpolar core of the cross-linked micelle. When hydrogen-bonding cross-linkers such as MBAm are introduced, they need to stay at the surfactant/water interface to be solvated by water. This layer of amide bonds, being quite polar, can interfere with the hydrophobic interactions because they cause discontinuity in hydrophobicity. According to our binding data, DVB was a better choice in such a situation. Not only does the aromatic cross-linker provide uninterrupted hydrophobicity, it could also enhance the cross-linking density of the micellar core by its nonpolar nature and preference for the nonpolar core of the micelle.

The situation should be reversed when highly hydrophilic peptides are present, whose binding rely more on polar, hydrogen-bonding interactions.[29] Consistent with the hypothesis, all the amide-cross-linkers were better than DVB. It is also interesting to see that MBAm outperformed the DVB–MBAm combination. The hydrophobic tail of a surfactant is known to adopt a rich variety of conformation in a micelle, and chain reversal or looping allows the chain end to easily reach the water-rich Stern region.[30] MBAm is hydrophilic and has to stay at the interface. Thus, the "core-cross-linking" in the MBAm-cross-linked MINPs should not be homogeneously distributed throughout the micelle core but be concentrated near the surface. According to our binding data, such an arrangement, at least in the case of WKK, was more beneficial than having the cross-linking both in the nonpolar core and near the interface (with the DVB–MBAm combination).

Selectivity of Peptide-Binding MINPs. In biomolecular recognition, changing a single important residue in a peptide can totally change its biological properties. Thus, being able to differentiate structurally similar sequences is crucial to a peptide receptor.

Table 2 compares the binding properties of MINP(WKK) prepared with DVB and MBAm as the core-cross-linker, respectively. We varied the middle residue and studied the binding of a range of WXK to understand the effect of the amide cross-linker on the recognition. Our data shows that the templating peptide (WKK) was bound more strongly by both MINPs than all the analogues, consistent with successful imprinting. Meanwhile, MINP(WKK) prepared with MBAm afforded significantly higher binding constant (5.4 times) than that with DVB. The difference in binding free energy (-Δ*G*) was ~1 kcal/mol (entry 1).

Table 2. Binding constants for different peptide guests by MINP(WKK) prepared with MBAm and DVB as the core-cross-linker.[a]

Entry	Guest	K_a ($\times 10^5$ M^{-1})		CRR		ΔΔ*G* (kcal/mol)	
		MBAm	DVB	MBAm	DVB	MBAm	DVB
1	WKK	17.8 ± 6.66	3.31 ± 0.37	1	1	0.00	0.00
2	WRK	6.11 ± 0.23	2.95 ± 0.43	0.34	0.89	0.63	0.07
3	WHK	6.85 ± 0.44	2.15 ± 0.51	0.38	0.65	0.57	0.26
4	WDK	8.10 ± 0.50	2.43 ± 0.62	0.45	0.73	0.47	0.18
5	WNK	5.64 ± 0.41	0.985 ± 0.04	0.32	0.30	0.68	0.72
6	WSK	4.24 ± 0.36	1.30 ± 0.12	0.24	0.40	0.85	0.55
7	WTK	2.86 ± 0.26	2.26 ± 0.45	0.16	0.68	1.08	0.23
8	WGK	3.56 ± 0.58	1.75 ± 0.71	0.20	0.52	0.95	0.38
9	WAK	6.97 ± 0.35	1.83 ± 0.81	0.39	0.55	0.56	0.35

[a] Titrations were performed in HEPES buffer (10 mM, pH 7.4) in duplicates at 298 K and the errors between the runs were <10%. CRR is the cross-reactivity ratio, defined as the binding constant of a guest relative to that of the templating peptide for a particular MINP. ΔΔ*G* = Δ*G*(guest) - Δ*G*(template).

The amide-functionalized MINP was superior not only in binding affinity but also in selectivity. Table 2 includes a column for CRR (cross-reactivity ratio), defined as the binding constant of a guest relative to that of the templating peptide for a particular MINP. The smaller the CRR value, the weaker was the

binding for the structural analogue, and the more selective was the MINP. The middle lysine (K) in the template (WKK) was basic. When the lysine was replaced with another basic residue (R or H), an acidic one (D), a hydrophilic polar residue (S or T), a hydrogen (G), or a small hydrophobic residue (A), the CRR value was always smaller for MINP made with MBAm than that with DVB. The only exception was asparagine (N), which had similar CRRs for the two MINPs. In every single case, the MBAm-derived MINP(WKK) could detect a single variation of the peptide, generally with $\Delta\Delta G \geq 0.5$ kcal/mol. The proposed interfacial hydrogen bonds should be the key reason for the improvements, as the DVB-derived MINP showed (not only weaker binding, but also) poorer selectivities.

To understand the generality of the interfacial-hydrogen-bonds-enhanced binding, we performed similar cross-reactivity studies using MINPs prepared with WDK (Table S1) and WTK (Table S2). A graphic comparison of the two cross-linkers is shown in Figure 2a (for WDK) and Figure 2b (for WTK). The middle amino acid is acidic in WDK and polar/nonionic in WTK, in contrast to the basic lysine in the middle of WKK. Importantly, the amide-functionalized MINPs displayed stronger binding affinities for their templates consistently (Tables S1–S2) and, in the vast majority of cases, higher selectivities among structural analogues (Figure 2). We also determined the imprinting factors by measuring the binding of WDK (Figure S10j) and WTK (Figure S12j) by the NINP. The MINP/NINP ratio remained extremely large, ~10000 for WDK and 3700 for WTK.

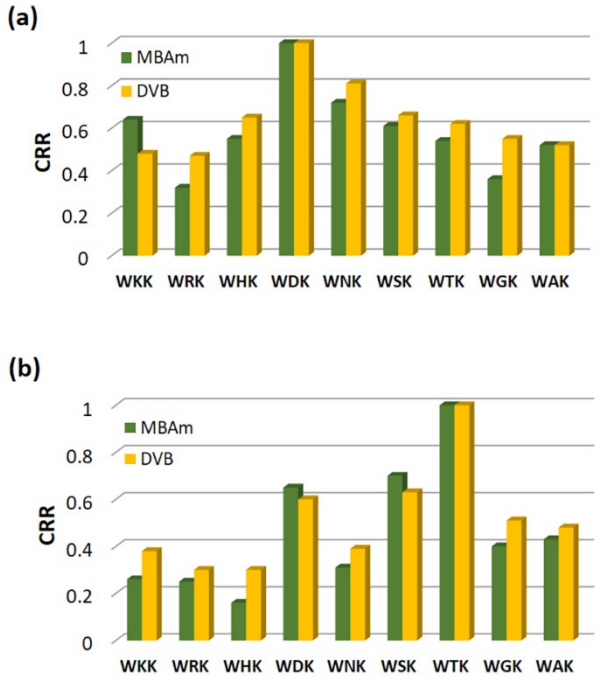

Figure 2. Comparison of CRR values for MINPs prepared with MBAm and DVB as the core-cross-linker using WDK (a) and WTK (b) as the template. See Tables S1 and S2 for the corresponding binding data.

One way to enhance the binding affinities of DVB-cross-linked MINP is through the inclusion of functional monomers that target specific side chains. Although this strategy cannot be applied to every side chain, it is effective for acidic and basic residues including glutamic acid (E), aspartic acid (D), lysine (K), and arginine (R) using FMs such as **10** and **11**.[31-33]

Following previously established protocols,[33] we prepared MINPs for WDK using MBAm and DVB as the core-cross-linker, respectively, with and without the FM **10** and **11** (Scheme 2). We studied the binding for the template (WDK), as well as a model guest (WRK), by ITC and summarized the results in Table 3.

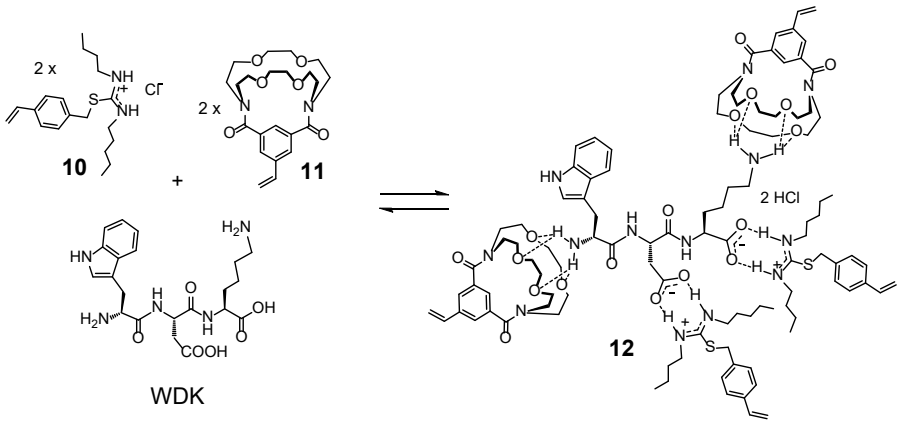

Scheme 2. Formation of hydrogen-bonded complex **12** from WDK and FMs **10** and **11** in micelle.

Table 3. Binding properties of MINPs prepared under different conditions for the templating peptide (WDK) and a model guest (WRK).[a]

entry	guest	cross-linker	FMs[b]	K_a ($\times 10^5$ M^{-1})	-ΔG (kcal/mol)	CRR
1	WDK	DVB	yes	9.02 ± 0.7	8.12	-
2			no	3.42 ± 0.41	7.54	-
3		MBAm	yes	11.0 ± 1.1	8.24	-
4			no	9.01 ± 0.82	8.12	-
5	WRK	DVB	yes	0.36 ± 0.03	6.21	0.04
6			no	1.60 ± 0.59	7.10	0.46
7		MBAm	yes	0.77 ± 0.02	6.66	0.07
8			no	2.89 ± 0.57	7.44	0.32

[a] Titrations were performed in HEPES buffer (10 mM, pH 7.4) in duplicates at 298 K and the errors between the runs were <10%. [b] For MINPs prepared with FMs, the following stoichiometry was used in the formulation: 1.5:1 for **10**/carboxylate and 1:1 for **11**/amine.

As shown by entries 1–2, inclusion of FM increased the binding for the template by 2.6 times. Meanwhile, the binding for the guest decreased from $K_a = 1.60 \times 10^5$ M^{-1} (entry 6) to 0.36×10^5 M^{-1} (entry

5), thus decreasing the CRR value from 0.46 (without FMs) to 0.04 (with FMs). The functional monomers, hence, strengthened the binding of the template while weakening that of the structural analogue, improving both the binding affinity and selectivity of the MINP as a result.

The functional monomers played a similar role for MBAm-derived MINP (Table 3, entries 3, 4, 7, 8). What is notable is that the binding constant for the templating peptide by MINP prepared without the FMs was 9.01×10^5 M^{-1} (entry 4), essentially the same as that by MINP with DVB and FMs (entry 1). In other words, MBAm, by its hydrogen-bonding capabilities, acted as a "functional cross-linker" to imprint the polar side chains as effectively as the FMs in the DVB-cross-linked MINP, at least in terms of binding affinity. Understandably, adding additional FMs in such a case brought little improvement (entry 3), as these FMs had to compete with the amide cross-linkers for the template. On the other hand, the benefit of FMs was in the selectivity, when MINP(WDK) was used to bind WRK (entries 7–8). Overall, although the selectivity was better for MBAm-cross-linked MINP than for DVB-cross-linked MINP in the absence of FMs, the highest selectivity was always obtained with the FMs.

Recognition of Biological Peptides. Our last set of experiments focused on hydrophilic biological peptides rich in polar groups (**13**–**18**, Figure 3). For each peptide, we prepared MINPs with DVB and FMs, as well as MINPs with MBAm without FMs (Table 4). The purpose of the study was to understand whether the amide-cross-linker could replace the FMs to yield competitive binding affinities. For practical applications, it is far more desirable to use a commercially available cross-linker (MBAm) instead of special FMs prepared through multistep synthesis.

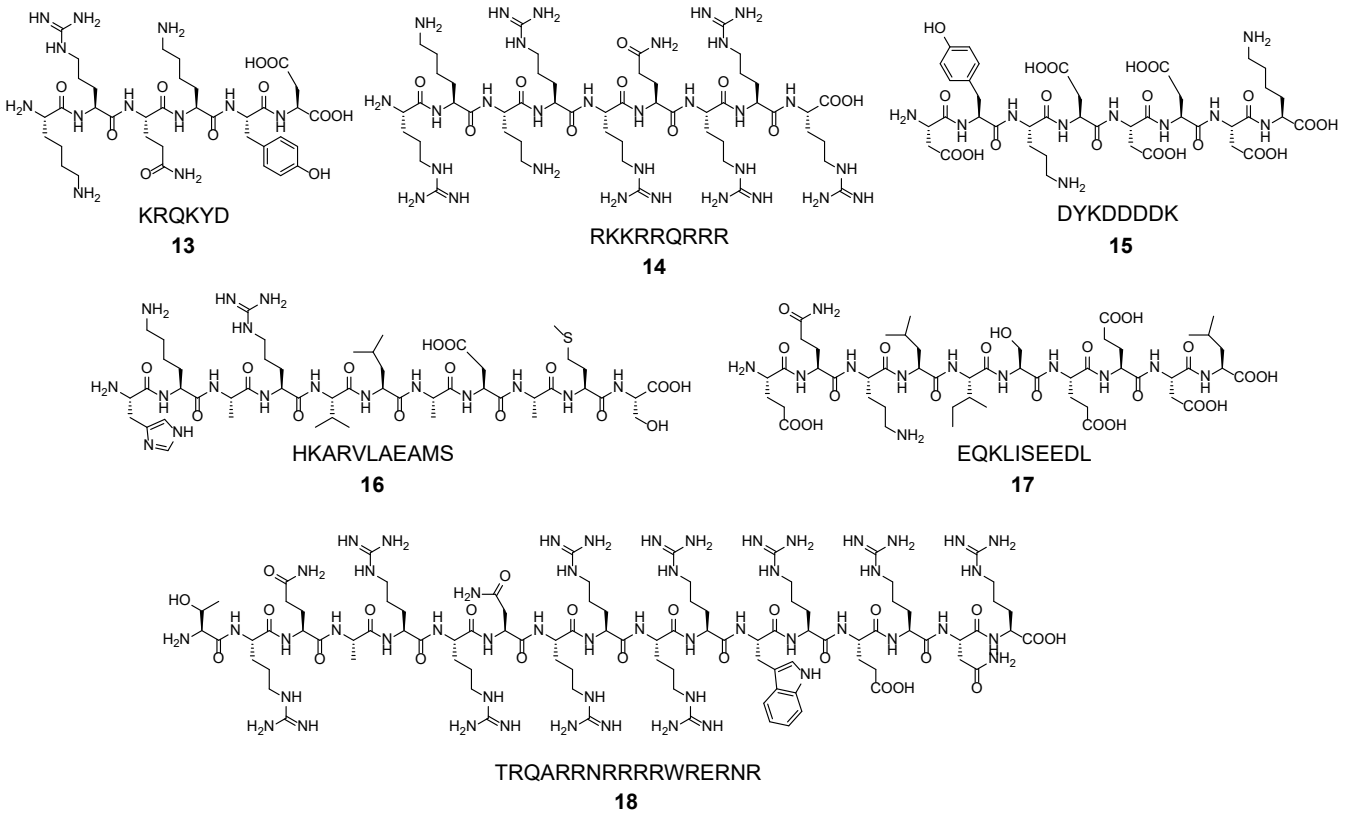

Figure 3. Structures of biological peptides **13**–**18** studied in this work.

Table 4. Binding data for biological peptides **13**–**18** by MINPs prepared with DVB and FMs, and by MINPs prepared with MBAm without FMs.[a]

entry	template	cross-linker	K_a ($\times 10^5$ M^{-1})	-ΔG (kcal/mol)	-ΔH (kcal/mol)	TΔS (kcal/mol)	N[b]
1	**13**	DVB	34.4 ± 1.73	8.91	23.28 ± 0.27	-14.38	0.9 ± 0.1
2		MBAm	62.2 ± 2.32	9.26	28.93 ± 0.22	-19.67	0.9 ± 0.1
3	**14**	DVB	45.3 ± 2.85	9.07	29.28 ± 0.32	-20.21	1.1 ± 0.1
4		MBAm	67.50 ± 2.66	9.31	23.16 ± 0.21	-13.85	1.1 ± 0.1
5	**15**	DVB	59.2 ± 0.31	9.23	31.60 ± 0.26	-22.37	1.1 ± 0.1
6		MBAm	73.10 ± 2.47	9.36	47.53 ± 0.33	-38.17	1.2 ± 0.1
7	**16**	DVB	82.3 ± 2.29	9.43	61.03 ± 0.33	-51.6	0.9 ± 0.1
8		MBAm	89.10 ± 2.47	9.47	64.94 ± 0.60	-55.47	1.1 ± 0.1
9	**17**	DVB	66.4 ± 2.65	9.30	34.20 ± 0.55	-24.9	0.8 ± 0.1

10		MBAm	72.50 ± 1.27	9.35	60.70 ± 1.07	-51.35	0.9 ± 0.1
11		DVB	53.40 ± 1.84	9.17	31.98 ± 0.25	-22.81	1.1 ± 0.1
12	**18**	MBAm	66.20 ± 3.36	9.30	35.98 ± 0.43	-26.68	1.0 ± 0.1

[a] The titrations were performed in HEPES buffer (10 mM, pH 7.4) in duplicates at 298 K and the errors between the runs were <10%. For MINPs prepared with FMs, the following stoichiometry was used in the formulation: 1.5:1 for **10**/carboxylate, 1:1 for **11**/amine, and 1:1 for **11**/arginine. [b] *N* is the number of binding sites per nanoparticle determined by ITC.

Gratifyingly, the MBAm-cross-linked MINPs consistently outperformed the DBV-cross-linked ones, despite the FMs added in the latter cases. The binding constants for **13**–**18** ranged from 60 to 90 $\times 10^5$ M^{-1}, translating to 110–170 nM of binding affinity in 10 mM HEPES buffer. Another noticeable trend in Table 4 is that all the bindings were enthalpically driven. Classical hydrophobic interactions are considered entropically driven, particularly at low temperatures,[34] but the thermodynamic details can change depending on the aliphatic/aromatic nature of the guests and the size/shape of the hydrophobic surfaces.[28,35,36] In our case, the driving force for the binding was rather complex, with contributions from a number of sources including hydrophobic interactions, hydrogen bonds, and electrostatic interactions.

We also examined the selectivity of the MINPs for the biological peptides. Figure 4 shows a cross reactivity study, with the biological peptides **13**–**18** titrated into a solution of MINP(**14**) and MINP(**17**), respectively. According to the ITC titration curves, in both cases, the templating peptide was bound by the MINP with excellent selectivity. While the desired peptide underwent large exothermic interactions with its corresponding MINP, the other peptides displayed very weak or negligible binding.

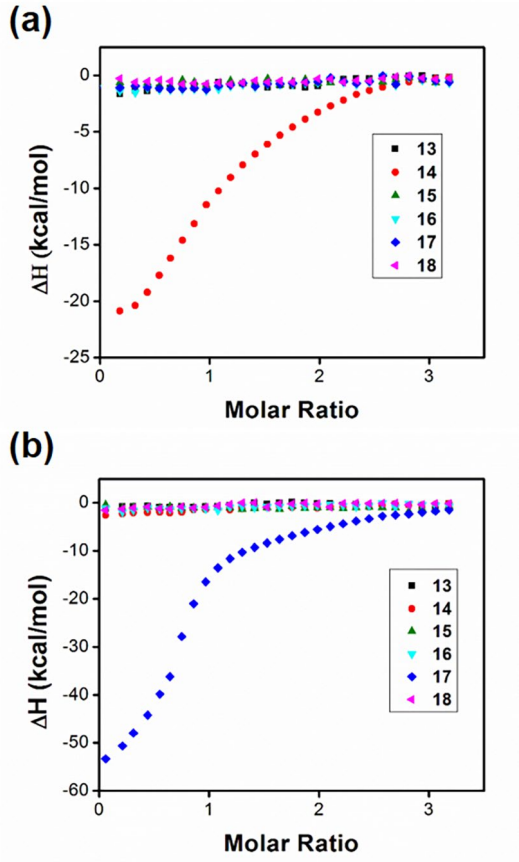

Figure 4. (a) ITC titration of peptides **13**–**18** to MINP(**14**), showing only the desired peptide bound by the MINP. (b) ITC titration of peptides **13**–**18** to MINP(**17**), showing only the desired peptide bound by the MINP. [MINP] = 5.0 μM. [peptide] = 75 μM in 10 mM HEPES buffer. The MINPs were prepared with 1:1 [**1**]/[MBAm].

Conclusions

Importance of peptide recognition in biology demands a simple and facile method to prepare their receptors. Whereas stepwise synthesis of molecular receptors becomes too complicated for long peptides, molecular imprinting within doubly cross-linked micelles provides a highly efficient way to prepare water-soluble peptide-binding nanoparticle receptors. MINP is a powerful platform to construct receptors for biomolecules including small-molecule drugs[37-39] and carbohydrates.[40,41] In this work, a simple change of the core-cross-linker from DVB to MBAm was found to enhance the binding affinities and selectivity for peptides substantially, through the interfacial hydrogen bonds formed between the cross-linked micelles and the peptide guests. MBAm was the best among the amide cross-linkers examined, possibly

because it represented a good balance of rigidity/flexibility and contained both hydrogen bond donors and acceptors. Being commercially available is an added benefit, as no extra synthesis was required. Importantly, an extremely large imprinting effect was observed, with imprinting/nonimprinting ratio in binding ranging from 3000 to 10000 for the model tripeptides. In addition, single variation in the tripeptide sequence was easily detected by the MBAm-cross-linked MINPs, much better than those prepared without the added amide bonds. Functional monomers were still very useful in enhancing the binding selectivity of MINPs. In cases where selectivity was not a limiting factor, MBAm could act as a hydrogen-bonding functional cross-linker to replace specially designed functional monomers, thus simplifying the preparation of artificial peptide receptors significantly.

Experimental Section

Syntheses of compounds **1**–**3**,[22] **10**[33] and **11**[33] were previously reported.

N,N'-(Ethane-1,2-diyl)bis(2-methylacrylamide) (4). A solution of methacryloyl chloride (1.07 mL, 11 mmol) in dichloromethane (5 mL) was added dropwise to N,N′-dimethylethylenediamine (0.54 mL, 5 mmol) and triethylamine (1.52 mL, 11 mmol) in dichloromethane (30 mL) at 0 °C under N_2. The reaction mixture was warmed to room temperature and stirred for 18 h. A solution of 0.5 M HCl (5 mL) was added. The organic phase was washed with water (2 × 20 mL), dried over Mg_2SO_4, and concentrated *in vacuo* to give the product as a yellow oil (0.8 g, 82%). ^{1}H NMR (400 MHz, $CDCl_3$, δ): 4.92 (br, 2H), 4.76 (br, 2H), 3.42 (s, 2H), 2.86 (s, 6H), 1.67 (s, 6H). ^{13}C NMR (100 MHz, $CDCl_3$, δ): 171.6, 141.1, 115.0, 43.5, 36.7, 20.2 ppm. ESI-QTOF-HRMS (m/z): $[M + H]^+$ calcd for $C_{12}H_{21}N_2O_2$ 225.1558; found, 225.1565.

N,N'-(Ethane-1,2-diyl)diacrylamide (5). Acryloyl chloride (0.9 mL, 11 mmol) in dichloromethane (5 mL) was added dropwise to a solution of N,N′-dimethylethylenediamine (0.54 mL, 5 mmol) and triethylamine (1.52 mL, 11 mmol) in dichloromethane (30 mL) at 0 °C under N_2. The reaction mixture was warmed to room temperature and stirred for 18 h. A solution of 0.5 M HCl (5 mL) was added. The organic phase was washed with water (2 × 20 mL), dried over Mg_2SO_4, and concentrated *in vacuo* to give

the product as a yellow oil (0.96 g, 86%). ^{1}H NMR (400 MHz, DMSO-d_6, δ): 6.67 (m, 2H), 6.07 (m, 2H), 5.62 (m, 2H), 3.50 (m, 4H), 3.01 (s, 3H), 2.86 (s, 3H). ^{13}C NMR (100 MHz, DMSO-d_6, δ): 165.9, 165.5, , 128.7, 128.3, 127.7, 127.3, 46.6, 44.9 ppm. ESI-QTOF-HRMS (m/z): $[M + H]^+$ calcd for $C_{10}H_{17}N_2O_2$ 197.1245; found, 197.1247.

1,1'-(Piperazine-1,4-diyl)bis(prop-2-en-1-one) (6). Acryloyl chloride (0.9 mL, 11 mmol) in dichloromethane (5 mL) was added dropwise over 15 min to piperazine (0.43 g, 5 mmol) and triethylamine (1.52 mL, 11 mmol) at 0 °C under N_2. The reaction mixture was warmed to room temperature and stirred for 18 h. A solution of 0.5 M HCl (5 mL) was added. The organic phase was washed with water (2 × 20 mL), dried over Mg_2SO_4, and concentrated in vacuo to give the product as yellow crystals (0.76 g, 78%). ^{1}H NMR (400 MHz, DMSO-d_6, δ): 6.80 (dd, J = 5 and 3 Hz, 2H), 6.12 (dd, J = 4 and 0.5 Hz, 2H), 5.69 (dd, J = 3 and 0.5 Hz, 2H), 3.57 (br, 8H). ^{13}C NMR (100 MHz, DMSO-d_6, δ): 164.8, 128.5, , 128.1, 45.6, 45.1, 42.1, 41.5 ppm. ESI-QTOF-HRMS (m/z): $[M + H]^+$ calcd for $C_{10}H_{15}N_2O_2$ 195.1089; found, 195.1199.

N'-Acryloylacrylohydrazide (8). Acryloyl chloride (0.89 mL, 11 mmol) was added dropwise over 5 min to hydrazine hydrate (0.26 mL, 5 mmol) and potassium carbonate (2.07 g, 15 mmol) in acetonitrile (15 mL) at 0 °C under N_2. The reaction mixture was warmed to room temperature and stirred for 4 h. The solid was removed by suction filtration and the filter cake was washed with dichloromethane (10 mL). The combined filtrate was concentrated in vacuo and the residue was purified by column chromatography over silica gel using 10:1 dichloromethane/methanol as the eluent to give the product as a purple powder (0.43 g, 62%). ^{1}H NMR (400 MHz, $CDCl_3$, δ): 10.2 (br, 2H), 6.27 (m, 4H), 5.58 (m, 2H). ^{13}C NMR (100 MHz, $CDCl_3$, δ): 163.2, 129.6, 127.3 ppm. ESI-QTOF-HRMS (m/z): $[M + H]^+$ calcd for $C_6H_9N_2O_2$ 141.0619; found, 141.0625.

N,N-Bis(2-acrylamidoethyl)acrylamide (9). Acryloyl chloride (1.4 mL, 17 mmol) was added dropwise over 5 min to diethylenetriamine (0.54 mL, 5 mmol) and potassium carbonate (2.76 g, 20 mmol) in acetonitrile (15 mL) at 0 °C under N_2. The reaction mixture was warmed to room temperature and stirred for 4 h. The solid was removed by suction filtration and the filter cake was washed with

dichloromethane (10 mL). The combined filtrate was concentrated in vacuo and the residue was purified by column chromatography over silica gel using 5:1 dichloromethane/methanol as the eluent to give the product as a yellow oil (1.1 g, 80%). ^{1}H NMR (400 MHz, DMSO-d_6, δ): 8.27 (t, J = 2 Hz, 1H), 8.22 (t, J = 2 Hz, 1H), 6.71 (dd, J = 4 and 2 Hz, 1H), 6.10 (m, 5H), 5.62 (dd, J = 4 and 1 Hz, 1H), 5.58 (m, 2H). ^{13}C NMR (100 MHz, DMSO-d_6, δ): 165.9, 165.5, , 165.2, 132.0, 131.8, 128.5, 127.8, 125.9, 125.6, 47.3, 46.2, 38.3, 37.0 ppm. ESI-QTOF-HRMS (m/z): $[M + H]^+$ calcd for $C_{13}H_{20}N_3O_3$ 266.1460; found, 266.1481.

Preparation of MINPs. To a micellar solution of compound **1** (9.3 mg, 0.02 mmol) in H_2O (2.0 mL), divinylbenzene (DVB, 2.8 μL, 0.02 mmol), desired peptide in H_2O (10 μL of a solution of 0.04 mmol/mL, 0.0004 mmol), and 2,2-dimethoxy-2-phenylacetophenone (DMPA,10 μL of a 12.8 mg/mL solution in DMSO, 0.0005 mmol) were added. The mixture was subjected to ultrasonication for 10 min before compound **2** (4.13 mg, 0.024 mmol), $CuCl_2$ (10 μL of a 6.7 mg/mL solution in H_2O, 0.0005 mmol), and sodium ascorbate (10 μL of a 99 mg/mL solution in H_2O, 0.005 mmol) were added. After the reaction mixture was stirred slowly at room temperature for 12 h, compound **3** (10.6 mg, 0.04 mmol), $CuCl_2$ (10 μL of a 6.7 mg/mL solution in H_2O, 0.0005 mmol l), and sodium ascorbate (10 μL of a 99 mg/mL solution in H_2O, 0.005 mmol) were added. After being stirred for another 6 h at room temperature, the reaction mixture was transferred to a glass vial, purged with nitrogen for 15 min, sealed with a rubber stopper, and irradiated in a Rayonet reactor for 12 h. The reaction mixture was poured into acetone (8 mL). The precipitate was collected by centrifugation and washed with a mixture of acetone/water (5 mL/1 mL) three times, methanol/acetic acid (5 mL/0.1 mL) three times, and acetone (6 mL) once before it was dried in air to afford the final MINPs as an off-white powder (16 mg, 80%). Similar procedures were followed for the amide-functionalized MINPs when **4**–**9** were used instead of DVB.

Determination of Binding Constants by ITC. ITC was performed on a MicroCal VP-ITC Microcalorimeter with Origin 7 software and VPViewer2000 (GE Healthcare, Northampton, MA), following standard procedures.[42-44] In general, a solution of an appropriate guest in Millipore water was injected in equal steps into 1.43 mL of the corresponding MINP in the same solution. The top panel shows

the raw calorimetric data. The area under each peak represents the amount of heat generated at each ejection and is plotted against the molar ratio of the MINP to the guest. The smooth solid line is the best fit of the experimental data to the sequential binding of N binding site on the MINP. The heat of dilution for the guest, obtained by titration carried out beyond the saturation point, was subtracted from the heat released during the binding. Binding parameters were auto-generated after curve fitting using Microcal Origin 7.

ASSOCIATED CONTENT

Supporting Information

The Supporting Information is available free of charge on the ACS Publications website.

ITC titration curves, additional figures, and NMR spectra of key compounds (PDF).

AUTHOR INFORMATION

Corresponding Author

*E-mail: zhaoy@iastate.edu

Notes

The authors declare no competing financial interest.

Acknowledgments

We thank NSF (DMR2002659) for financial support of this research

References

(1) Peczuh, M. W.; Hamilton, A. D. Peptide and Protein Recognition by Designed Molecules. *Chem. Rev.* **2000**, *100*, 2479-2494.

(2) Maity, D.; Schmuck, C.: Chapter 8 Synthetic Receptors for Amino Acids and Peptides. In *Synthetic Receptors for Biomolecules: Design Principles and Applications*; The Royal Society of Chemistry, 2015; pp 326-368.

(3) van Dun, S.; Ottmann, C.; Milroy, L.-G.; Brunsveld, L. Supramolecular Chemistry Targeting Proteins. *J. Am. Chem. Soc.* **2017**, *139*, 13960-13968.

(4) Klein, J. U.; Whitcombe, M. J.; Mulholland, F.; Vulfson, E. N. Template-Mediated Synthesis of a Polymeric Receptor Specific to Amino Acid Sequences. *Angew. Chem. Int. Ed.* **1999**, *38*, 2057-2060.

(5) Urraca, J. L.; Aureliano, C. S. A.; Schillinger, E.; Esselmann, H.; Wiltfang, J.; Sellergren, B. Polymeric Complements to the Alzheimer's Disease Biomarker B-Amyloid Isoforms Aβ1–40 and Aβ1–42 for Blood Serum Analysis under Denaturing Conditions. *J. Am. Chem. Soc.* **2011**, *133*, 9220-9223.

(6) Hoshino, Y.; Kodama, T.; Okahata, Y.; Shea, K. J. Peptide Imprinted Polymer Nanoparticles: A Plastic Antibody. *J. Am. Chem. Soc.* **2008**, *130*, 15242-15243.

(7) Hoshino, Y.; Koide, H.; Urakami, T.; Kanazawa, H.; Kodama, T.; Oku, N.; Shea, K. J. Recognition, Neutralization, and Clearance of Target Peptides in the Bloodstream of Living Mice by Molecularly Imprinted Polymer Nanoparticles: A Plastic Antibody. *J. Am. Chem. Soc.* **2010**, *132*, 6644-6645.

(8) Rachkov, A.; Minoura, N. Towards Molecularly Imprinted Polymers Selective to Peptides and Proteins. The Epitope Approach. *Biochim. Biophys. Acta, Protein Struct. Mol. Enzymol.* **2001**, *1544*, 255-266.

(9) Nishino, H.; Huang, C. S.; Shea, K. J. Selective Protein Capture by Epitope Imprinting. *Angew. Chem. Int. Ed.* **2006**, *45*, 2392-2396.

(10) Bossi, A. M.; Sharma, P. S.; Montana, L.; Zoccatelli, G.; Laub, O.; Levi, R. Fingerprint-Imprinted Polymer: Rational Selection of Peptide Epitope Templates for the Determination of Proteins by Molecularly Imprinted Polymers. *Anal. Chem.* **2012**, *84*, 4036-4041.

(11) Yang, K.; Liu, J.; Li, S.; Li, Q.; Wu, Q.; Zhou, Y.; Zhao, Q.; Deng, N.; Liang, Z.; Zhang, L.; Zhang, Y. Epitope Imprinted Polyethersulfone Beads by Self-Assembly for Target Protein Capture from the Plasma Proteome. *Chemical Communications* **2014**, *50*, 9521-9524.

(12) Zhang, Y.; Deng, C.; Liu, S.; Wu, J.; Chen, Z.; Li, C.; Lu, W. Active Targeting of Tumors through Conformational Epitope Imprinting. *Angew. Chem. Int. Ed.* **2015**, *54*, 5157-5160.

(13) Li, S.; Yang, K.; Deng, N.; Min, Y.; Liu, L.; Zhang, L.; Zhang, Y. Thermoresponsive Epitope Surface-Imprinted Nanoparticles for Specific Capture and Release of Target Protein from Human Plasma. *ACS Appl. Mater. Interfaces* **2016**, *8*, 5747-5751.

(14) Schwark, S.; Sun, W.; Stute, J.; Lutkemeyer, D.; Ulbricht, M.; Sellergren, B. Monoclonal Antibody Capture from Cell Culture Supernatants Using Epitope Imprinted Macroporous Membranes. *RSC Adv.* **2016**, *6*, 53162-53169.

(15) Pan, G.; Shinde, S.; Yeung, S. Y.; Jakštaitė, M.; Li, Q.; Wingren, A. G.; Sellergren, B. An Epitope‐Imprinted Biointerface with Dynamic Bioactivity for Modulating Cell–Biomaterial Interactions. *Angew. Chem. Int. Ed.* **2017**, *56*, 15959-15963.

(16) Qin, Y.-P.; Jia, C.; He, X.-W.; Li, W.-Y.; Zhang, Y.-K. Thermosensitive Metal Chelation Dual-Template Epitope Imprinting Polymer Using Distillation–Precipitation Polymerization for Simultaneous Recognition of Human Serum Albumin and Transferrin. *ACS Appl. Mater. Interfaces* **2018**, *10*, 9060-9068.

(17) Xing, R.; Ma, Y.; Wang, Y.; Wen, Y.; Liu, Z. Specific Recognition of Proteins and Peptides Via Controllable Oriented Surface Imprinting of Boronate Affinity-Anchored Epitopes. *Chem. Sci.* **2019**, *10*, 1831-1835.

(18) Thielmann, Y.; Weiergräber, O. H.; Mohrlüder, J.; Willbold, D. Structural Framework of the Gabarap–Calreticulin Interface–Implications for Substrate Binding to Endoplasmic Reticulum Chaperones. *The FEBS journal* **2009**, *276*, 1140-1152.

(19) Pettersen, E. F.; Goddard, T. D.; Huang, C. C.; Couch, G. S.; Greenblatt, D. M.; Meng, E. C.; Ferrin, T. E. UCSF Chimera--a Visualization System for Exploratory Research and Analysis. *J. Comput. Chem.* **2004**, *25*, 1605-1612.

(20) Chothia, C.; Janin, J. Principles of Protein-Protein Recognition. *Nature* **1975**, *256*, 705-708.

(21) Davis, A. M.; Teague, S. J. Hydrogen Bonding, Hydrophobic Interactions, and Failure of the Rigid Receptor Hypothesis. *Angew. Chem. Int. Ed.* **1999**, *38*, 736-749.

(22) Awino, J. K.; Zhao, Y. Protein-Mimetic, Molecularly Imprinted Nanoparticles for Selective Binding of Bile Salt Derivatives in Water. *J. Am. Chem. Soc.* **2013**, *135*, 12552-12555.

(23) A water-soluble peptide also has a significant driving force to associate with a micelle because their hydrophobic side chains prefer to be buried in a hydrophobic microenvironment instead of being exposed to water.

(24) Awino, J. K.; Gunasekara, R. W.; Zhao, Y. Sequence-Selective Binding of Oligopeptides in Water through Hydrophobic Coding. *J. Am. Chem. Soc.* **2017**, *139*, 2188-2191.

(25) Wulff, G. Molecular Imprinting in Cross-Linked Materials with the Aid of Molecular Templates—a Way Towards Artificial Antibodies. *Angew. Chem. Int. Ed. Engl.* **1995**, *34*, 1812-1832.

(26) Schmidtchen, F. P.: Isothermal Titration Calorimetry in Supramolecular Chemistry. In *Supramolecular Chemistry: From Molecules to Nanomaterials*; Steed, J. W., Gale, P. A., Eds.; Wiley: Weinheim, 2012.

(27) Chen, K.; Zhao, Y. Effects of Nano-Confinement and Conformational Mobility on Molecular Imprinting of Cross-Linked Micelles. *Org. Biomol. Chem.* **2019**, *17*, 8611-8617.

(28) Tanford, C.: *The Hydrophobic Effect: Formation of Micelles and Biological Membranes*; 2nd ed.; Krieger: Malabar, Fla., 1991.

(29) Although water molecules in the binding sites would also be displaced in such a case, hydrogen bonds between the host (i.e., the amides) and the guest (the peptide) clearly would be more important in the latter case.

(30) Menger, F. M.; Doll, D. W. On the Structure of Micelles. *J. Am. Chem. Soc.* **1984**, *106*, 1109-1113.

(31) Fa, S.; Zhao, Y. Water-Soluble Nanoparticle Receptors Supramolecularly Coded for Acidic Peptides. *Chem. -Eur. J.* **2018**, *24*, 150-158.

(32) Fa, S.; Zhao, Y. Peptide-Binding Nanoparticle Materials with Tailored Recognition Sites for Basic Peptides. *Chem. Mater.* **2017**, *29*, 9284-9291.

(33) Fa, S.; Zhao, Y. General Method for Peptide Recognition in Water through Bioinspired Complementarity. *Chem. Mater.* **2019**, *31*, 4889-4896.

(34) Abraham, M. H. Free Energies, Enthalpies, and Entropies of Solution of Gaseous Nonpolar Nonelectrolytes in Water and Nonaqueous Solvents. The Hydrophobic Effect. *J. Am. Chem. Soc.* **1982**, *104*, 2085-2094.

(35) Blokzijl, W.; Engberts, J. B. F. N. Hydrophobic Effects - Opinions and Facts. *Angew. Chem. Int. Ed. Engl.* **1993**, *32*, 1545-1579.

(36) Southall, N. T.; Dill, K. A.; Haymet, A. D. J. A View of the Hydrophobic Effect. *J. Phys. Chem. B* **2002**, *106*, 521-533.

(37) Awino, J. K.; Zhao, Y. Polymeric Nanoparticle Receptors as Synthetic Antibodies for Nonsteroidal Anti-Inflammatory Drugs (NSAIDs). *ACS Biomater. Sci. Eng.* **2015**, *1*, 425-430.

(38) Duan, L.; Zhao, Y. Selective Binding of Folic Acid and Derivatives by Imprinted Nanoparticle Receptors in Water. *Bioconjugate Chem.* **2018**, *29*, 1438-1445.

(39) Duan, L.; Zhao, Y. Zwitterionic Molecularly Imprinted Cross-Linked Micelles for Alkaloid Recognition in Water. *J. Org. Chem.* **2019**, *84*, 13457-13464.

(40) Awino, J. K.; Gunasekara, R. W.; Zhao, Y. Selective Recognition of D-Aldohexoses in Water by Boronic Acid-Functionalized, Molecularly Imprinted Cross-Linked Micelles. *J. Am. Chem. Soc.* **2016**, *138*, 9759-9762.

(41) Gunasekara, R. W.; Zhao, Y. A General Method for Selective Recognition of Monosaccharides and Oligosaccharides in Water. *J. Am. Chem. Soc.* **2017**, *139*, 829-835.

(42) Wiseman, T.; Williston, S.; Brandts, J. F.; Lin, L. N. Rapid Measurement of Binding Constants and Heats of Binding Using a New Titration Calorimeter. *Anal. Biochem.* **1989**, *179*, 131-137.

(43) Jelesarov, I.; Bosshard, H. R. Isothermal Titration Calorimetry and Differential Scanning Calorimetry as Complementary Tools to Investigate the Energetics of Biomolecular Recognition. *J. Mol. Recognit.* **1999**, *12*, 3-18.

(44) Velazquez-Campoy, A.; Leavitt, S. A.; Freire, E. Characterization of Protein-Protein Interactions by Isothermal Titration Calorimetry. *Methods Mol. Biol.* **2004**, *261*, 35-54.

TOC graphic